# The FliN−FliH Interaction Mediates Localization of Flagellar Export ATPase FliI to the C Ring Complex†

Jonathan L. McMurry,*,‡ James W. Murphy,§ and Bertha González-Pedrajo||

*Department of Molecular Biophysics and Biochemistry, Yale University, New Haven, Connecticut 06520-8114, Department of Pharmacology, Yale University School of Medicine, New Haven, Connecticut 06520-8066, and Departamento de Genética Molecular, Instituto de Fisiología Celular, Universidad Nacional Autónoma de México, Ap. Postal 70-243, México D.F. 04510, México*

*Received March 24, 2006; Revised Manuscript Received July 31, 2006*

ABSTRACT: FliH regulates the flagellar export ATPase FliI, preventing nonproductive ATP hydrolysis. FliH has been shown to stably associate with the C ring protein FliN. Analysis of this complex reveals that FliH is required for FliI localization to the C ring, and thus FliH not only inhibits FliI ATPase activity but also may act to target FliI to the basal body. Quantitative binding studies revealed a $K_D$ of 110 nM for FliH binding to FliN. The $K_D$ for FliH binding of a FliN variant from a temperature-sensitive nonflagellate *fliN* point mutant was determined to be 270 nM, suggesting a molecular explanation for its phenotype. Another variant FliN from a temperature-sensitive mutant with a different phenotype displayed binding with an intermediate affinity. Weak export activity in a *fliN* null mutant was greatly increased by overproduction of FliI, mimicking a previously observed FliH bypass effect and supporting the conclusion that FliN−FliH binding is important for localization of FliI to the C ring and thus the membrane-embedded export apparatus beyond. A model incorporating the present findings is presented.

The bacterial flagellum is a complex, self-assembling molecular machine responsible for motility in many species (*1, 2*). At least 34 proteins are either structural components of the flagellum or necessary for its assembly. With a few exceptions, flagellar proteins reach their destinations via a dedicated type III export apparatus contained within the basal body of the flagellum (*3, 4*). In *Salmonella enterica* serovar Typhimurium, this apparatus consists of six membrane proteins (FlhA, FlhB, FliO, FliP, FliQ, and FliR), likely housed in a patch of membrane within the MS ring,[1] and three soluble proteins (FliH, FliI, and FliJ).

Flagellar export begins after formation of the MS ring and probably commensurate with formation of the C ring. Following export, substrates diffuse through a continuous interior channel within the nascent flagellum to their final location (*5, 6*)

FliI is an ATPase which couples ATP hydrolysis to translocation of export substrates across the CM (*7*), perhaps by catalyzing chaperone release and unfolding of substrates, as occurs with FliI virulence ortholog InvC (*8*). FliH is a negative regulator of FliI ATPase activity. FliH and FliI form a $(FliH)_2FliI$ heterotrimer which presumably prevents nonproductive ATP hydrolysis (*9, 10*). Both FliI and FliH have been shown to interact with FlhA and FlhB by affinity blotting, FRET, and isolation of intergenic pseudorevertants (*11*−*13*).

FliG, FliM, and FliN form the C ring which functions as the flagellar rotor and contains the directional switching capability of the motor. Purified FliM−FliN complexes from *Thermotoga maritima* possessed a $FliM_1-FliN_4$ ratio (*14*), in reasonable agreement with that observed by quantitative immunoblots of *Salmonella* basal bodies, from which an estimate of a $FliG_{44}-FliM_{35}-FliN_{110}$ stoichiometry was made (*15*). All three proteins can assemble onto the cytoplasmic side of the MS ring in the absence of the export apparatus (*16*). Null mutants of all three genes are nonflagellate (*fla*) (*17*−*19*). However, the roles of the C ring proteins are varied; mutants thereof can have paralyzed, nonchemotactic, or nonflagellate phenotypes (*20, 21*).

*fliN*$^{ts}$ mutant MY669 failed to export all external flagellar proteins at the restrictive temperature (*22*). Another *fliN*$^{ts}$ mutant, SJW2284, was immotile and unable to regrow flagella after shearing at the restrictive temperature, which led to a proposal of an indirect role for FliN in export (*23*). Overexpression and underexpression of *fliN* in *Escherichia coli* caused defects in both motility and flagellation (*17*).

*Yersinia pestis* virulence secretion apparatus proteins YscL and YscQ, orthologous to FliH and FliN, respectively, were identified as binding partners in a yeast two-hybrid screen (*24*). An interaction was also observed between MxiN and

† This work was primarily conducted in the laboratory of Robert M. Macnab, who passed away in 2003. It was supported by Public Health Service grants AI12202 (originally awarded to R.M.M.) and GM070333 (J.L.M.).

* To whom correspondence should be addressed. Department of Chemistry & Biochemistry, Kennesaw State University, 1000 Chastain Road, MB# 1203, Kennesaw, GA 30144. E-mail: jmcmurr1@kennesaw.edu.

‡ Yale University.

§ Yale University School of Medicine.

|| Universidad Nacional Autónoma de México.

[1] CM, cytoplasmic membrane; CCW, counterclockwise; DTT, dithiothreitol; FRET, fluorescence resonance energy transfer; IMAC, immobilized metal affinity chromatography; IPTG, isopropyl-β-D-thiogalactopyranoside; MCS, multiple cloning site; MS, membrane−supramembrane; ts, temperature sensitive.

10.1021/bi0605890 CCC: $33.50 
Published on Web 09/12/2006

Table 1: Strains and Plasmids Used in This Study

| strain/plasmid | relevant characteristic | source or reference |
|---|---|---|
| | *E. coli* Strains | |
| BL21(DE3) | for overproduction of proteins | Novagen |
| BL21(DE3)pLysS | for overproduction of proteins | Novagen |
| NovaBlue | recipient for cloning experiments | Novagen |
| | *Salmonella* Strains | |
| JR501 | $r^-m^-$; for making plasmids *Salmonella* compatible | (*43*) |
| SJW1103 | wild-type for motility | (*44*) |
| SJW2284 | temperature-sensitive *fliN* mutant | (*23*) |
| MY669 | temperature-sensitive *fliN* mutant | (*22*) |
| MKM10 | Δ*fliH*[a] | (*32*) |
| MKM15 | Δ*fliN* | (*27*) |
| MKM65 | Δ*fliR* | (*45*) |
| | Plasmids | |
| pET19b | N-terminal His-tag T7 expression vector | Novagen |
| pTrc99A | expression vector | Amersham (*46*) |
| pTrc99AFF4 | modified pTrc expression vector[b] | (*47*) |
| pACTrc | pTrc promoter, p15A origin of replication[c] | (*27*) |
| pGMK3000 | pET19b His-FliG[d] | (May Kihara, unpublished) |
| pMMK4310 | pTrc99A His-FliM−FliN[e] | (May Kihara, unpublished) |
| pBGGhMN | pTrc99AFF4 FliG/His-FliM + FliN[f] | (*27*) |
| pACTrcHI | pACTrc FliH + FliI[g] | (*27*) |
| pACTrcI | pACTrc FliI | (Gillian Fraser, unpublished) |
| pMM309 | pTrc FliH | (*9*) |
| pMM1702 | pTrc99A His-FliI | (*9*) |
| pJM341 | pET19b HisFliM + FliN(N:L89Q) | this study |
| pJM342 | pET19b HisFliM + FliN(N:V87G) | this study |
| pJM349 | pTrc99A HisFliM + FliN(N:V113D)[h] | this study |
| pJM358 | pTrc99A HisFliM + FliN(N:V111D)[h] | this study |
| pJM359 | pTrc99A HisFliM + FliN(N:V112D)[h] | this study |

[a] Identical to MKM11, which is described in ref 32. [b] pTrc99AFF4 is modified from pTrc99A to remove the NdeI site at 2699−2704 and change the NcoI site in the MCS to an NdeI site, which allows for shuttling of inserts from pTrc99AFF4 to pET19b by restriction with NdeI and BamHI. [c] pACTrc is a homemade expression vector (Gillian Fraser) that is derived from pACYC184 (New England Biolabs). It was produced by insertion of SphI−EcoRV and EcorRV−HindIII fragments from pTrc99AFF4 into pACYC184, yielding a plasmid of 5240 bp. Its p15A origin of replication and $Cm^r$ allow for cotransformation with pET- and pTrc-based plasmids. [d] *fliG* was amplified from the chromosome using oligos containing NdeI and BamHI sites and cloned into pET19b. [e] Contains *fliM* and *fliN*, which are immediately adjacent on the *Salmonella* chromosome, as one fragment amplified from chromosomal DNA. The insert was first cloned into pET19b via NdeI and BamHI and then shuttled to pTrc99A by restricting with NcoI and BamHI so that the pET19b-derived sequence coding for a His-tag was retained. Thus, pMMK4310 codes for His-FliM and untagged FliN expressed from the same trc promoter. [f] *fliG* was cloned into NdeI and BamHI sites. Genes for FliM and FliN were shuttled as one insert from pET19b by restriction with XbaI and HindIII, both of which are in the pTrc99AFF4 MCS. The resultant insert has *fliM* and *fliN* with an additional pET19b-derived sequence coding for an N-terminal His-tag on FliM and a ribosomal binding site. [g] *fliH* and *fliI* were cloned into pACTrcHI by taking advantage of their immediately adjacent positions on the *Salmonella* chromosome. Thus, one fragment containing both genes was cloned into NdeI and BamHI sites and both were expressed from the same trc promoter. [h] Mutations were made in *fliN* as described in the methods. A single insert containing both *fliM* and *fliN* (with a His-tag encoded FliM) was cloned into pTrc99A via NcoI and BamHI.

Spa33 (FliH and FliN orthologs) from *Shigella flexneri* (*25*). That study found that a *mxiN* mutant was unable to form a needle, though it did form a normal basal structure. These findings constitute strong evidence for a role for FliN in export and suggest that it may be a receptor for FliH.

Structures of *Thermotoga maritima* FliN and the C-terminal domain of its paralog, HrcQB, from *Pseudomonas syringae* have been solved (*14*, *26*). *Thermotoga* FliN possesses a conserved surface-exposed hydrophobic patch. A mutation altering one of the residues in the patch caused reduced flagellation and a CCW motor bias, alluding to potential roles for the patch in both switching and export (*14*). Other site-directed mutations caused flagellation defects, some of which were alleviated by overproduction of FliH and FliI (K. Paul, J. Harmon, D. Blair, personal communication).

González-Pedrajo et al. (*27*) reported copurification of *Salmonella* FliH with FliN. Herein, that interaction is demonstrated to be specific and quantitatively characterized. A FliN variant from a ts mutant is shown to bind more weakly to FliH, suggesting that the FliN−FliH interaction plays an important role in export and providing a molecular explanation for the mutant phenotype. Additionally, a previously reported "bypass" effect of FliI overproduction in a *fliH* null was mimicked in a *fliN* null mutant background. We propose that FliH not only is a negative regulator of FliI ATPase activity but also localizes FliI to the basal body.

## EXPERIMENTAL PROCEDURES

*Strains and Media.* Bacterial strains and plasmids used in this study are listed in Table 1. pACTrc is an expression vector derived from pACYC184 that contains $lacI^q$, a trc promoter and MCS from pTrc99AFF4, yielding a plasmid providing chloramphenicol resistance and having the same MCS as pTrc99AFF4 (Gillian Fraser, personal communication). Because of their different origins of replication, pACTrc and pTrc99AFF4 are compatible for coexpression. All cultures were grown in Luria broth (LB). Ampicillin (50 $\mu g\ mL^{-1}$) and chloramphenicol (25 $\mu g\ mL^{-1}$) were added where appropriate.

*DNA Manipulations.* Chromosomal DNA was prepared by the method of Woo et al. (*28*). Mutations were made in *fliN* to create plasmids pJM341, pJM342, pJM349, pJM358, and

pJM359 by a method adapted from Toker et al. (*29*). Briefly, complementary primers coding for the mutation were paired with outside primers to amplify fragments using Pfu Turbo DNA polymerase (Stratagene, La Jolla, CA) and pMMK4310 (pTrc99A/His-FliM−FliN) as the template. Sequences for primers used to produce plasmids first described in this study are listed in Supporting Information Table 1. Products were gel purified and used as templates for a second round of amplification with the outside primers that produced one fragment containing the full-length *fliM* and *fliN* genes with the altered codon in *fliN*. These products were gel purified, restricted with NdeI and BamHI, and cloned into pET19b. To create pJM349, pJM358, and pJM359, the pET19b parent was restricted with NcoI and BamHI. The insert was gel purified and cloned into pTrc99A using NovaBlue cells, resulting in plasmids coding for His-FliM and FliN variants. The correct sequence was confirmed prior to use (W. M. Keck Foundation Biotechnology Resources Laboratory at Yale University).

*Copurification Experiments.* Coexpression and purification experiments were performed essentially as described using pTrc- and pACTrc-based plasmids as needed (*10*). Briefly, a 25 mL culture of BL21(DE3) cells transformed with one or two plasmids was grown at 30 °C to an $OD_{600}$ of 0.4. IPTG was added to a final concentration of 0.2 mM, and growth continued for 2 h. Cells were then harvested, resuspended in 10 mL of lysis buffer (50 mM Tris, pH 8.0, 500 mM NaCl, 10 mM imidazole), and sonicated. A clarified lysate was produced by centrifugation at 10 000*g* for 20 min followed by centrifugation of the supernatant at 100 000*g* for 1 h. The lysate was then loaded by gravity flow onto a 1 mL Talon (BDBiosciences Clontech, Palo Alto, CA) IMAC column, washed with 20 mL of wash buffer (50 mM Tris, pH 8.0, 500 mM NaCl, 25 mM imidazole), and eluted in 3 × 1 mL fractions in elution buffer (50 mM Tris, pH 8.0, 500 mM NaCl, 250 mM imidazole). A sample from fraction 2 was taken for SDS−PAGE analysis of copurified proteins.

*Purification of His-FliM−FliN Complexes for Binding Studies.* An overnight culture of *E. coli* BL21(DE3)pLysS carrying pMMK4310, pJM341, pJM342, pJM349, pJM358, or pJM359 was subcultured 1:100 into 500 mL of LB. The culture was grown with vigorous shaking at 30 °C until it reached an $OD_{600}$ of 0.4. IPTG was then added to a final concentration of 0.2 mM, and growth continued for 4 h. Cells were harvested by centrifugation and stored at −85 °C.

Cell pellets were thawed on ice, resuspended in 50 mL of lysis buffer (50 mM Tris, pH 8.0, 500 mM NaCl, 10 mM imidazole), sonicated, and centrifuged at 10 000*g* for 20 min. The supernatant was then centrifuged at 100 000*g* for 1 h. The second supernatant was loaded by gravity flow onto a 5 mL Talon IMAC column, washed with 20 column volumes of wash buffer (50 mM Tris, pH 8.0, 500 mM NaCl, 25 mM imidazole), and eluted in the elution buffer (50 mM Tris, pH 8.0, 500 mM NaCl, 250 mM imidazole). Eluted fractions were pooled, concentrated, loaded, and run on a Superdex-200 HR 10/30 gel filtration column (Amersham Pharmacia, Piscataway, NJ) equilibrated and run in 20 mM Tris, pH 8.0, 150 mM NaCl, 1 mM DTT, and 1 mM EDTA. Protein eluted in two peaks, one containing a high molecular weight contaminant and the other containing only FliM−FliN complexes. The latter was collected and concentrated for binding studies.

*Saturation Binding Assays*. To determine the affinity of FliH for FliN, a saturation binding assay was developed using quantitative immunoblotting. A portion of 10 $\mu$g/mL (final concentration) of the His-FliM−FliN complex was mixed with varying amounts of a lysate of BL21(DE3)pLysS producing untagged FliH from pMM309 produced as described above in a final volume of 1 mL of lysis buffer. (For the FliH−FliI binding experiment, a lysate of BL21(DE3) cells overproducing FliH and FliI from pACTrcHI was used.) The mixture was incubated at 25 °C for 1 h, after which 50 $\mu$L of a 50% slurry of Talon resin equilibrated in lysis buffer was added. Binding was allowed to continue for another 1 h with gentle mixing for a total of 2 h. The resin was pelleted via brief centrifugation and washed twice with 1 mL of wash buffer. The bound protein was then eluted by addition of 50 $\mu$L of elution buffer. Eluted protein was briefly spun to remove any resin, mixed with sample buffer, boiled, and run on 15% SDS−PAGE gels.

Proteins were transferred to nitrocellulose and immunoblotted with polyclonal anti-FliH antisera (gift of G. Schoenhals) using chemiluminescent detection. Experiments were performed in triplicate. Triplicate blots were exposed to the same sheet of film for the same length of time, usually 2−5 s. Background-subtracted band densities were measured using ImageJ version 1.33u (W. S. Rasband, NIH, http://rsb.info.nih/gov/ij). The points on the saturation curves represent the mean ± SEM. Data were fit to a one-binding site hyperbola ($Y = B_{max}*[FliH]/(K_D + [FliH])$) by nonlinear regression with GraphPad Prism (GraphPad Software, San Diego, CA). $B_{max}$, the value representing maximal binding of FliH to FliN, was determined by extrapolation from densitometry values and was used solely to calculate $K_D$. The values of $B_{max}$ between experiments with different FliN variants depended on several experimental factors including blot exposure time and are not directly comparable even though the concentration of His-FliM−FliN complexes remained constant. $K_D$ was determined to be the value of [FliH] at half of the calculated $B_{max}$. Plots were normalized to percent maximal binding where $100\% = B_{max.}$

The concentration of FliH in the lysate was measured by immunoblotting against a standard curve of purified His-FliH. The contribution of the His-tag to the molecular weight of the standards was accounted for in determining the concentration of lysate FliH.

Polyclonal antisera for FliM, FliN (gifts of S.-I. Aizawa), and FliI (*30*) were used in blots of saturation binding samples to ascertain retention of those proteins in the complexes. Control experiments with His-FliM only, no His-FliM−FliN, and with BL21(DE3)pLysS lysate without FliH were performed to ensure that FliH binding to resin-bound FliN was specific and that His-FliM−FliN repurification was constant at all quantities of added lysate. No FliH binding to the resin was detected within the limits of the assays.

*Export Assays*. Export assays were performed essentially as described (*27*) using polyclonal anti-FlgD antisera (*31*).

## RESULTS

*Association of FliI with the C Ring Protein Complex Requires FliH*. FliH and FliI interact with each other (*9*, *10*), but it was unknown if FliI stably interacts with any C ring proteins. González-Pedrajo et al. copurified FliH with a

complex of C ring proteins FliG, FliM, and FliN via interaction with FliN and purified a complex of FliG, FliM, FliN, FliH, and FliI (*27*). That study also demonstrated that the C-terminal domain of FliN (residues 58−137) binds FliH in copurification experiments but did not examine FliI−C ring protein interactions. To determine whether FliG, FliM, or FliN had interactions with FliI, we produced combinations of these proteins by overproduction from one or two plasmids in BL21(DE3) and subjected them to copurification attempts (Supporting Information, Figure 1). Our results showed that none of the C ring proteins had a detectable interaction with FliI and that only FliN (in complex with FliM) bound FliH. FliM and FliN were always expressed together to ensure stability and solubility; FliM itself does not bind FliH (*27*). These results, taken together with those of González-Pedrajo et al., suggest that FliI is localized to the basal body by interaction with FliH, which binds FliN.

*The FliN−FliH Interaction Is Specific.* To analyze the interaction between FliN and FliH, a saturation binding assay was developed. Purified His-FliM−FliN, which had an apparent molecular mass of about 140 kDa by gel filtration, was measured by multiangle light scattering to be 120 kDa (data not shown), consistent with a complex from *Thermotoga maritima* that had a stoichiometry of $FliM_1-FliN_4$ (*14*). The *T. maritima* complex also eluted from gel filtration with an apparent mass of 140 kDa but was found by sedimentation equilibrium analytical ultracentrifugation to be 98.6 ± 3.5 kDa (calculated *T. maritima* $FliM_1-FliN_4$ mass = 98.5 kD). Our His-FliM and FliN have predicted molecular masses of 40.6 and 14.8 KDa, respectively. A His-$FliM_1-FliN_4$ complex would thus have a mass of 99.8 kDa. Although a His-$FliM_2-FliN_2$ complex (110.8 kDa) is also consistent with the measured mass and we cannot rule it out, we consider $FliM_1-FliN_4$ the more likely stoichiometry because of the similarity to the *T. maritima* complex; FliN has an elongated shape (*14*) that likely results in the anomalously large gel filtration elution position.

Complexes were mixed with various amounts of a clarified lysate containing a known concentration of untagged FliH. The mixture was incubated at 25 °C for 2 h with gentle mixing. The His-FliM−FliN with bound FliH was then repurified. Samples were run on 15% SDS−PAGE gels, transferred to nitrocellulose, and subjected to immunoblotting using anti-FliH antisera. No FliH bound to the resin in parallel experiments performed with His-FliM alone or no His-tagged protein; i.e., under experimental conditions, all detectable FliH binding to FliN was specific (data not shown).

Figure 1A shows a typical anti-FliH blot used for saturation binding analysis. The same samples blotted with anti-FliM and anti-FliN demonstrate that the His-FliM−FliN complex is retained under experimental conditions and that the quantities remain constant in all samples (Figure 1B). His-FliM−FliN was retained in all samples in a parallel experiment with a BL21(DE3)pLysS lysate that did not contain FliH; i.e., the lysate did not cause dissociation of FliN from His-FliM or interfere with the binding of His-FliM−FliN to the resin (data not shown). Figure 1C shows the saturation binding curve from which the $K_D$ was calculated to be 110 ± 20 nM. The Hill coefficient is 1.1 ± 0.2, indicating noncooperativity (Figure 1C, inset).

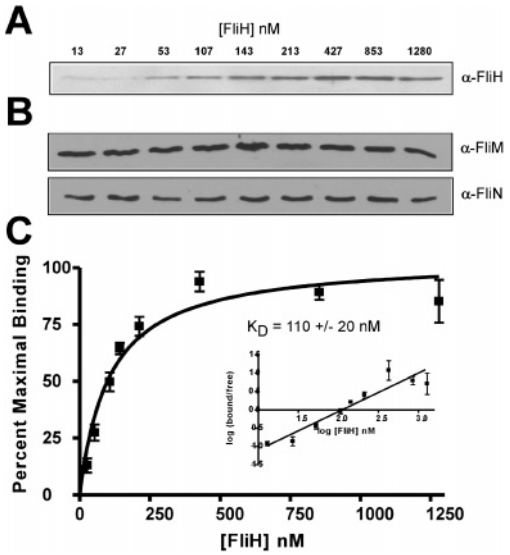


FIGURE 1: FliH saturation binding assay for wild-type FliN. (A) Representative anti-FliH immunoblot of repurified His-FliM−FliN−FliH complexes. The concentration of FliH in each sample is shown above each lane. (B) Anti-FliM and anti-FliN immunoblots of the same samples in A. (C) Saturation binding curve generated from the mean of three experiments ± SEM. Inset: Hill plot of saturation binding data.

*FliH−FliI Complexes Bind FliN.* Saturation analysis of FliN binding to FliH when in the presence of FliI in an overexpressed lysate was performed (Figure 2). The FliH−FliI lysate was produced from pACTrcHI. Quantitation of FliH between lysates was subject to experimental error, and thus the $K_D$ was not directly comparable to the FliH-only lysate used for determination of $K_D$ for FliN−FliH. However, FliI-bound FliH (see Discussion) demonstrated saturation at concentrations similar to FliH only and occurred with a concomitant increase in density of FliI bands in the same samples (Figure 2A). The Hill coefficient is 1.1 ± 0.1, indicating noncooperativity (Figure 2B, inset). Although the specificity of the anti-FliI antibody was insufficient to determine a pseudo-$K_D$ (FliI itself does not bind FliN) under the same conditions used to measure FliH−FliN binding, the pattern of increasing FliI band density parallels that of FliH (Figure 2B), strongly suggesting that FliH−FliI complexes bind to FliN in a manner similar to FliH alone.

*FliN from a ts Mutant Has Altered Affinity for FliH.* Temperature-sensitive *fla fliN* mutant strains MY669 and SJW2284 have been described (*22, 23*). The entire *fliN* gene was amplified from chromosomal DNA prepared from the mutants and sequenced. Both were found to be single-base substitution mutations. MY669 contains a T260G substitution, which codes for FliN with a V87G replacement. SJW2284 contains T266A that codes for L89Q.

FliH saturation binding analysis was performed with the two FliN variants coded by the mutations coproduced from pJM341 and pJM342 and purified in complex with His-FliM in the same manner as for wild-type FliN (Figure 3A and 3B). Both His-FliM and FliN were retained as shown for the wild-type (Figure 1B), indicating that the variants did not differ in FliM binding (data not shown). The $K_D$ for FliH binding by FliN(V87G) is 270 ± 60 nM (Figure 3A), which is noticeably weaker than the wild-type. The $K_D$ for FliH binding by FliN(L89Q) is 190 ± 40 nM (Figure 3B), which is intermediate but weaker than the wild-type affinity. These

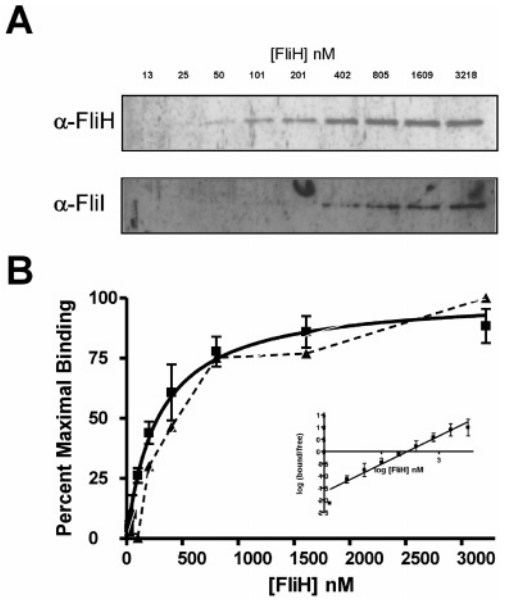


FIGURE 2: FliI-bound FliH saturation binding analysis of wild-type FliN. (A) Representative anti-FliH and anti-FliI immunoblots of repurified His-FliM−FliN−FliH−FliI complexes from the saturation binding assay. The concentration of FliH in each sample is shown above each lane. (B) Saturation binding curve for FliH (solid line) generated from the mean of three experiments ± SEM. The triangles represent anti-FliI band densities (normalized to densest band = 100%) in the immunoblot. The dotted line is intended as an aid for the eye only to demonstrate that the increase in FliI band density parallels that of FliH. Inset: Hill plot of FliH saturation binding data.

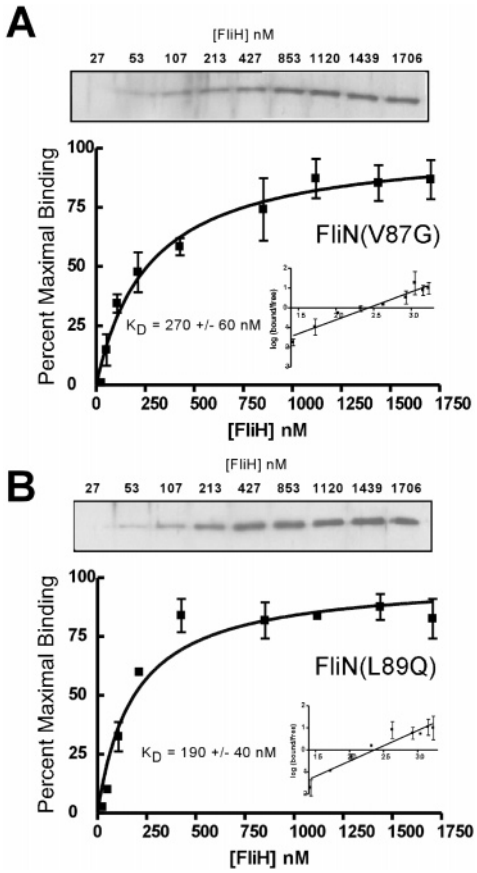


FIGURE 3: FliH saturation binding analysis with temperature-sensitive FliNs. (A) Representative anti-FliH blot and saturation binding analysis of repurified His-FliM−FliN(V87G)−FliH. The concentration of FliH in each sample is shown above each lane. The saturation binding curve was generated from the mean of three experiments ± SEM. Inset: Hill plot of saturation binding data. (B) Representative anti-FliH blot and saturation binding analysis of His-FliM−FliN(L89Q). The arrangement is the same as that in A.

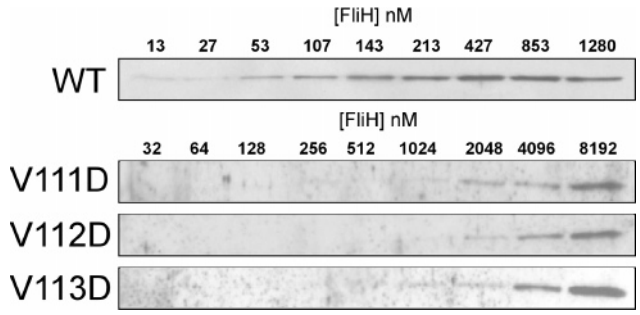


FIGURE 4: FliH binding analysis of FliN hydrophobic patch variants. (Top) Wild-type (WT) FliN is shown for comparison. (Bottom) Patch variants FliN(V111D), FliN(V112D), and FliN(V113D) were not saturated with FliH within the limits of the assay. The concentration of FliH in each sample is shown above each lane.

binding constants suggest a molecular explanation for the mutant phenotypes. Hill coefficients are 1.4 ± 0.2 for FliN(V87G) and 1.3 ± 0.2 for FliN(L89Q), suggesting noncooperativity (see Discussion).

*Disruption of the Surface-Exposed Hydrophobic Patch Reduces FliN Affinity for FliH*. Paul et al. showed that *E. coli* FliN variants with alterations in the conserved hydrophobic patch had flagellation defects (K. Paul, J. Harmon, and David Blair, personal communication). We made three of these variants in *Salmonella* FliN, FliN(V111D), FliN(V112D), and FliN(V113D) (*E. coli* and *Salmonella* FliNs are invariant from residues 52−137); overproduced them as His-FliM−FliN complexes from pJM349, pJM358, and pJM359; and purified and subjected them to FliH saturation binding analysis (Figure 4). Though binding was specific, saturation was not achieved within the limits of the assay; 8 $\mu$M was the FliH concentration in the undiluted lysate. Thus, a $K_D$ could not be determined, but the affinity is substantially weaker than that of the wild-type and the V87G and L89Q variants.

*A fliN Null Export Defect Is Alleviated by Overproduction of FliI*. Overproduction of FliI has been shown to alleviate export and motility defects in MKM10, a *fliH* null strain. Interestingly, MKM10, weakly motile at 30 °C, is immotile at 42 °C even in the presence of overproduced FliI (as are SJW2284 and MY669) (data not shown). Thus, attempts to mimic the bypass effect with the *fliN*$^{ts}$ mutants proved impossible because the effect does not occur at the restrictive temperature even in MKM10. However, *fliN* null MKM15 did exhibit the bypass effect (Figure 5). Overproduction of His-FliI from pMM1702 did not affect export of the hook-capping protein FlgD in wild-type strain SJW1103 nor lack thereof in the *fliR* null MKM65, which has a complete export defect (lanes 1−4). MKM15 exhibited very weak export when transformed with an empty vector but robustly exported FlgD when FliI was overproduced from pMM1702 (lanes 7 and 8), mimicking the FliH bypass in MKM10 (lanes 5 and 6). FlgD was detected at similar levels in all cells. Though export competent, MKM15 remained immotile upon overproduction of FliI, likely reflecting motor rotation defects due to the absence of FliN (data not shown).

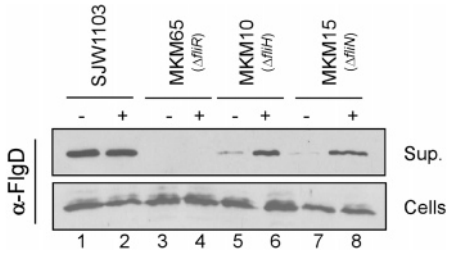


FIGURE 5: Effect of FliI overproduction on the export of hook-capping protein FlgD. Anti-FlgD immunoblots of culture supernatant (upper panel) and cell lysate (lower panel) in wild-type strain SJW1103 (lanes 1 and 2), *fliR* null MKM65 (lanes 3 and 4), *fliH* null MKM10 (lanes 5 and 6), and *fliN* null MKM15 (lanes 7 and 8). (−) Cells transformed with empty pTrc99A. (+) Cells transformed with pMM1702 (encoding His-FliI).

## DISCUSSION

Copurification and two-hybrid observations in flagellar (*27*) and other type III systems (*24, 25, 33*) have identified a FliN−FliH interaction. This study demonstrated that the interaction is specific, that binding is submicromolar in affinity, that FliN from a mutant defective for export has a weaker affinity for FliH, and that similar to the FliH bypass effect the export defect of a *fliN* null can be alleviated by overproduction of FliI. Thus, we suggest that FliH serves to localize FliI to the C ring, and likely the membrane apparatus, via interaction with FliN.

Mutations in all three C ring proteins can result in *fla* phenotypes. However, our results indicate that FliG and FliM do not participate directly in binding to FliH or FliI. It is likely that export defects in *fla, fliG, fliM,* and some *fliN* strains result indirectly from altered interactions among the C ring proteins themselves. These could lead to the absence of FliN from, or incorrect incorporation into, the C ring, resulting in failure of FliH to localize to the basal body. Interestingly, at the restrictive temperature, FliF (the MS ring protein) and probably FliP and FliQ incorporated into the basal body in *fliN*$^{ts}$ mutant MY669 (*22*). Our present results indicate that other membrane components are able to assemble in the absence of FliN because there is very weak export activity (Figure 5, lane 7). Thus, assembly of the membrane export apparatus components is probably not dependent on FliN, but efficient delivery of substrates to them is.

*Saturation Binding Assay*. This study is the first to quantitatively address binding of FliH to FliN. Copurification and two-hybrid assays, while informative, are potentially susceptible to nonspecific interactions. The saturability of FliH binding to His-FliM−FliN demonstrates specificity. We developed the binding assay using FliH lysates because we were unable to purify untagged FliH that was suitable for binding studies. Attempts to remove His-tags or to purify untagged FliH either failed or produced FliH that had an unacceptably high degree of nonspecific binding. Although determination of FliH concentration by immunoblots is suboptimal and subject to experimental error, the same FliH lysate was used in assay binding of all FliN variants. The $K_D$'s are thus comparable, and the relative affinities of the FliNs for FliH are V87G < L89Q < WT.

*FliH−FliN Binding in the Presence of FliI*. Using a lysate in which both FliH and FliI had been overproduced, FliI-bound FliH was shown to bind FliN in a manner similar to free FliH (Figure 2). Although the possibility that free FliH bound FliN and was in turn bound by FliI exists, several observations argue that free FliH was unlikely to be present in the lysate in any significant quantity. Overproduced FliH and His-FliI ran as a single band in native gels in which free FliI was not present in detectable quantities (*9*). In our measurements, FliI was present in excess of FliH relative to the $(FliH)_2FliI$ stoichiometry, suggesting that all FliH was in complex with FliI; FliH cannot displace FliI from His-FliH to which it had been previously bound suggesting that once bound dissociation is negligible under conditions nearly identical to those of the saturation binding assay (J. McMurry, unpublished observation). We suspect that the affinity of FliH for FliN is insensitive to the presence of FliI; development of a binding assay using purified untagged FliH and FliH−FliI will help resolve this issue.

*FliH−FliN Binding Is Not Cooperative*. The saturation binding curves presented herein are fit to single-site binding hyperbolae. They do not fit a two-site model. FliH forms a dimer, and *T. maritima* FliM−FliN complexes possess a $FliM_1-FliN_4$ stoichiometry (*14*). FliN−FliH binding might be expected to be cooperative. However, the Hill coefficient for FliH binding by FliN is close to 1 ($1.1 \pm 0.2$) for wild-type FliN, indicating that binding is not cooperative. We speculate that the FliN variants are also not cooperative and that their relatively higher Hill coefficients ($1.4 \pm 0.2$ and $1.3 \pm 0.2$) are the result of the limitations of the sensitivity of our assay and use of linear regression to analyze saturation binding data, though we cannot rule out a change in cooperativity. Interestingly, FliN binding to FliI-bound FliH is also not cooperative; the Hill coefficient is $1.1 \pm 0.1$. Whether binding within intact C rings or in the presence of ATP analogues, in which FliI forms homohexamers (*34*), would affect the cooperativity of FliH−FliN binding are important matters for future investigation.

*The Affinities of FliN Variants for FliH Correlate with the Phenotypes of the Mutants*. Prima facie, the difference in affinities of FliH for FliN between the two *fliN*$^{ts}$ mutants seems odd given the primary sequence and spatial proximity of the mutations. Indeed, more dramatic affinity differences may be present at 42 °C, but saturation binding at the restrictive temperature could not be carried out for technical reasons. However, there are differences in the phenotypes. The FliN(V87G) mutant, MY669, regained export function when shifted to the permissive temperature, but the FliN-(L89Q) mutant, SJW2284, failed to regrow filaments after shearing, was immotile even if not sheared after a shift to the restrictive temperature, and did not regain motility when shifted back to the permissive temperature (*22, 23*). Thus, the phenotype of MY669 might be explained solely by an altered FliN affinity for FliH, but the defect of SJW2284 may be viewed as more severe, perhaps due to other altered interactions.

It is unlikely that the FliN(V87G) and FliN(L89Q) variants directly disrupt the FliH binding site. An alignment of *Salmonella* FliN with *T. maritima* FliN and *Pseudomonas* HrcQB sequences is shown in Figure 6A. The residues making significant contributions to the surface-exposed hydrophobic patch are shown for *T. maritima.* The solvent-exposed surface of the *T. maritima* FliN is shown in Figure 6B. It demonstrates that I104 and L106, the residues corresponding to *Salmonella* V87 and L89, have very little

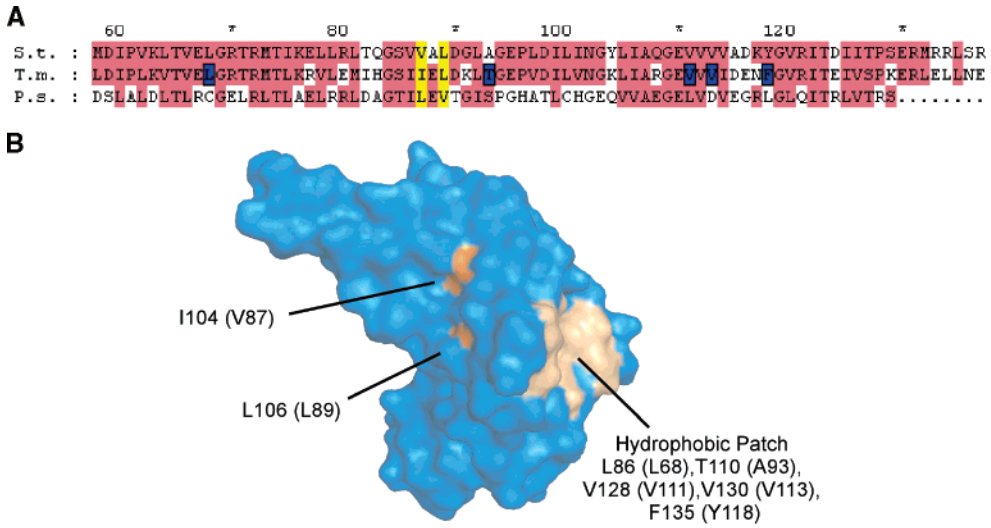


FIGURE 6: (A) Alignment of *Salmonella* FliN residues 58−137 and corresponding sequences from *Thermotoga maritima* FliN (residues 74−154) and *Pseudomonas syringae* HrcQB (57−128). *Salmonella* residue numbers are shown along the top. Highly conserved residues are highlighted in red. *Salmonella* V87 and L89 and corresponding residues are shown in yellow. Residues identified by Brown et al. (*14*) as being involved in the surface-exposed hydrophobic patch are boxed and highlighted in blue. (B) Structure of *T. maritima* FliN dimer (accession number 1YAB) with the hydrophobic patch surface shown in light brown. The surface exposed areas of I104 and L106 are shown in orange. The corresponding *Salmonella* residues are in parentheses. Hydrophobic patch residues are shown for both monomers. I104 and L106 are only shown for one chain. The structure was made using PyMol, version 0.99 (Delano Scientific LLC, http://pymol.sourceforge.net/).

surface exposure: only the backbone carbonyl oxygen of L106 is surface exposed, whereas the side chain of I104 is partially exposed. There is likely less surface exposure of V87 in *Salmonella* FliN owing to its shorter side chain. The bulk of the residues is buried and is underneath the hydrophobic surface patch. Thus we speculate that the variants exert their effects indirectly. Brown et al. made a mutation that resulted in a patch variant (V113D) that affected both flagellation and switching in a temperature-sensitive manner (*14*). As those authors noted, patch residues are conserved even in two species that do not have a chemotactic signaling pathway and whose FliN homologues are therefore uninvolved in switching, suggesting the possibility that the patch is a binding site for an export protein. That protein is likely FliH. Indeed, in FliH binding experiments utilizing FliN hydrophobic patch variants V111D, V112D, and V113D, all of which exhibit flagellation defects in vivo (K. Paul, J. Harmon, and David Blair, personal communication), saturation was not achieved within the limits of our assay (Figure 4). Thus, the $K_D$'s for FliH binding to these FliN variants are at least severalfold higher than those for the wild-type, supporting the hypothesis that the hydrophobic patch is the FliH binding site.

*FliN−FliH Interactions within the C Ring*. It is unlikely that every FliN within the C ring is occupied by FliH. An estimated 111 ± 13 copies of FliN are present in the C ring (*15*), probably well in excess of the number of FliH or FliH−FliI complexes involved in export at each basal body. Underexpression of FliN allowed for flagellar assembly but not rotation (*17*), demonstrating that the number of FliNs sufficient for export is less than that required for rotation. The position of FliN within the C ring remains a matter of some speculation. However, electron microscopic image reconstructions show a bulge at the bottom of the C ring into which FliN tetramers could fit (*35*). Perhaps the position of FliN within the C ring, the likely availability of unoccupied binding sites, and the moderate affinity (110 nM) for FliH serve well to localize FliH−FliI complexes to the C ring on their way to the membrane-integrated export apparatus components, conferring an entropic advantage without unduly detaining them with stronger binding.

FliI is capable of export sufficient for motility upon overexpression in a *fliH* null strain and export in a *fliN* null strain. Second-site "bypass" mutations of the *fliH* null were localized to *flhA* and *flhB* (*32*). FlhB and probably FlhA protrude from the interior of the C ring (J. McMurry and N. Francis, unpublished observation), likely constituting what has been described as the C rod (*36*). Perhaps less stable, lower affinity interactions with FlhA and FlhB are sufficient for export when FliI is overproduced, i.e., the state required for *fliH* and *fliN* null bypass effects, but FliH-mediated C ring localization is required for efficient export in the wild-type case where FliI concentrations are dramatically lower. FliI and FliH interactions with FlhA and FlhB shown by affinity blotting have been reported (*13*, *37*). There are a number of flagellar secretion systems for which there is no obvious FliH homologue (*3*). It is possible that the bypass effect seen by Minamino et al. (*32*) reflects how apparatuses probably lacking FliH, e.g., *Aquifex aeolicus*, operate.

*Model for Dynamic Interactions between the Export Apparatus and the C Ring.* Current findings and previously reported results are incorporated into a model (Figure 7). At the top of the schematic (Figure 7A) is the "resting state" in which $(FliH)_2FliI$ is bound to the C ring near its cytoplasmic face where FliN is likely located (*38*). In Figure 7B, an export substrate is delivered to $(FliH)_2FliI$, in this case by the general chaperone FliJ (*39*). FliH and FliJ copurify when overproduced (*40*). In Figure 7C, the $(FliH)_2FliI$−substrate complex dissociates from FliN and migrates to the cytoplasmic domains of FlhA and/or FlhB. The distance between the bottom of the C ring where FliH may bind FliN and the membrane, as much as 17 nm (*38*), is such that FliN−FliH dissociation is likely. The FliN−FliH interaction is dynamic; FliH competes for FliH−FliI binding to His-FliM−FliN (J.

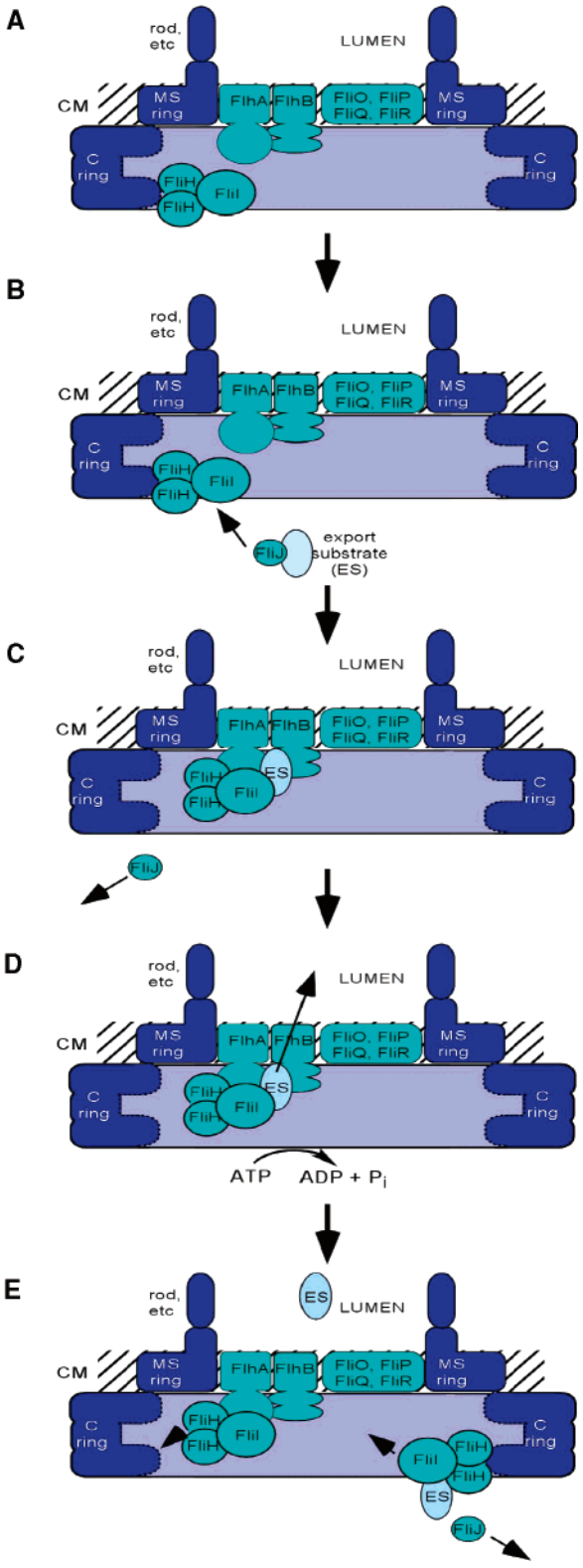


FIGURE 7: Model of export apparatus function incorporating FliN−FliH interactions. Flagellar structural components (C ring, MS ring, and rod) are dark blue. Export apparatus proteins are cyan. (A) The resting state in which $(FliH)_2FliI$ is bound to FliN at the bottom of the C ring. (B) The export substrate is delivered by general chaperone FliJ. (C) $(FliH)_2FliI$ export substrate dissociates from FliN and binds the membrane-bound export apparatus. (D) FliI-catalyzed ATP hydrolysis allows for export of the substrate across the CM into the flagellar lumen. (E) Post export, $(FliH)_2FliI$ shuttles back to FliN in preparation for receiving another substrate.

McMurry, unpublished observation). Interactions of FliH and FliI with the cytoplasmic domains of FlhA and FlhB have been observed (*13*, *37*). ATP hydrolysis by FliI in Figure 7D powers the translocation of the export substrate. Dissociation of the FlhA−FlhB−FliH−FliI complex post translocation would allow multiple FliI complexes to function. Another $(FliH)_2FliI$−substrate complex is shown dissociating from the C ring (Figure 7E).

Alternate possibilities abound. $(FliH)_2FliI$ may interact with chaperones and substrates in the cytoplasm prior to binding FliN. Indeed, stalled intermediate complexes of FliH, FliI, and variant chaperones that strongly bind their substrates have been detected in the cytoplasm (*41*). FliH may bind FliN in the absence of FliI. FliI may dissociate from FliN−FliH upon arrival of an export substrate and migrate to the membrane-bound export apparatus on its own; FliI has an affinity for lipids (*42*). Higher-order oligomers of FliH−FliI may play a role in export, particularly when FliI approaches the membrane-bound apparatus. FliI forms hexamers in vitro in the presence of nonhydrolyzable ATP analogues, and oligomerization of FliI is promoted by *E. coli* lipids (*34*); whether FliH participates in FliI oligomerization is unknown. There is evidence that FliJ binds to FlhA (*13*, *37*, *40*) suggesting that FliJ may remain in complex with FliH−FliI. Further investigation should shed significant light on the dynamics of flagellar export.

## ACKNOWLEDGMENT

We are deeply indebted to Robert M. Macnab, under whose leadership this project was begun. We gratefully acknowledge David Blair for helpful comments and sharing the *T. maritima* FliN structure prior to publication. We thank May Kihara for critical reading, editorial assistance, and construction of pMMK4310, Mark Tardie for assistance with multiangle light scattering, Gillian Fraser for construction of pACTrc, and John Van Arnam for technical assistance. We also thank Keiichi Namba, Tohru Minamino, and Hedda Ferris for helpful suggestions and critical reading of the manuscript.

## SUPPORTING INFORMATION AVAILABLE

Includes a table containing the sequences of oligonucleotides used to produce the plasmids described in this study and a figure demonstrating copurification of the C ring and export protein complexes. This material is available free of charge via the Internet at http://pubs.acs.org.

## REFERENCES

1. Macnab, R. M. (1996) Flagella and motility. In *Escherichia coli and Salmonella: Cellular and Molecular Biology* (Neidhardt, F. C., Curtiss, R., III, Ingraham, J. L., Lin, E. C. C., Low, K. B., Magasanik, B., Reznikoff, W. S., Riley, M., Schaechter, M., and Umbarger, H. E., Eds.) pp 123−145, ASM Press, Washington, DC.
2. Macnab, R. M. (2003) How bacteria assemble flagella, *Annu. Rev. Microbiol. 57*, 77−100.
3. Macnab, R. M. (2004) Type III flagellar protein export and flagellar assembly, *Biochim. Biophys. Acta 1694*, 207−217.
4. Minamino, T., and Namba, K. (2004) Self-assembly and type III protein export of the bacterial flagellum, *J. Mol. Microbiol. Biotechnol. 7*, 5−17.
5. Morgan, D. G., Macnab, R. M., Francis, N. R., and DeRosier, D. J. (1993) Domain organization of the subunit of the *Salmonella typhimurium* flagellar hook, *J. Mol. Biol. 229*, 79−84.
6. Mimori, Y., Yamashita, I., Murata, K., Fujiyoshi, Y., Yonekura, K., Toyoshima, C., and Namba, K. (1995) The structure of the

R-type straight flagellar filament of *Salmonella* at 9 Å resolution by electron cryomicroscopy, *J. Mol. Biol. 249*, 69−87.
7. Fan, F., and Macnab, R. M. (1996) Enzymatic characterization of FliI: an ATPase involved in flagellar assembly in *Salmonella typhimurium*, *J. Biol. Chem. 271*, 31981−31988.
8. Akeda, Y., and Galán, J. E. (2005) Chaperone release and unfolding of substrates in type III secretion, *Nature (London) 437*, 911−915.
9. Minamino, T., and Macnab, R. M. (2000) FliH, a soluble component of the type III flagellar export apparatus of *Salmonella*, forms a complex with FliI and inhibits its ATPase activity, *Mol. Microbiol. 37*, 1494−1503.
10. González-Pedrajo, B., Fraser, G. M., Minamino, T., and Macnab, R. M. (2002) Molecular dissection of *Salmonella* FliH, a regulator of the ATPase FliI and the type III flagellar protein export pathway, *Mol. Microbiol. 45*, 967−982.
11. Minamino, T., and Macnab, R. M. (1999) Components of the *Salmonella* flagellar export apparatus and classification of export substrates, *J. Bacteriol. 181*, 1388−1394.
12. Zhu, K., González-Pedrajo, B., and Macnab, R. M. (2002) Interactions among membrane and soluble components of the flagellar export apparatus of *Salmonella*, *Biochemistry 41*, 9516−9524.
13. McMurry, J. L., Van Arnam, J. S., Kihara, M., and Macnab, R. M. (2004) Analysis of the cytoplasmic domains of *Salmonella* FlhA and interactions with components of the flagellar export machinery, *J. Bacteriol. 186*, 7586−7592.
14. Brown, P. N., Mathews, M. A. A., Joss, L. A., Hill, C. P., and Blair, D. F. (2005) Crystal structure of the flagellar rotor protein FliN from *Thermotoga maritima*, *J. Bacteriol. 187*, 2890−2902.
15. Zhao, R., Pathak, N., Jaffee, H., Reese, T. S., and Khan, S. (1996) FliN is a major structural protein of the C-ring in the *Salmonella typhimurium* flagellar basal body, *J. Mol. Biol. 261*, 195−208.
16. Kubori, T., Yamaguchi, S., and Aizawa, S.-I. (1997) Assembly of the switch complex onto the MS ring complex of *Salmonella typhimurium* does not require any other flagellar proteins, *J. Bacteriol. 179*, 813−817.
17. Tang, H., Billings, S., Wang, X., Sharp, L., and Blair, D. F. (1995) Regulated underexpression and overexpression of the FliN protein of *Escherichia coli* and evidence for an interaction between FliN and FliM in the flagellar motor, *J. Bacteriol. 177*, 3496−3503.
18. Tang, H., and Blair, D. F. (1995) Regulated underexpression of the FliM protein of *Escherichia coli* and evidence for a location in the flagellar motor distinct from the MotA/MotB torque generators, *J. Bacteriol. 177*, 3485−3495.
19. Lloyd, S. A., Tang, H., Wang, X., Billings, S., and Blair, D. F. (1996) Torque generation in the flagellar motor of *Escherichia coli*: Evidence of a direct role for FliG but not FliM or FliN, *J. Bacteriol. 178*, 223−231.
20. Irikura, V. M., Kihara, M., Yamaguchi, S., Sockett, H., and Macnab, R. M. (1993) *Salmonella* typhimurium *fliG* and *fliN* mutations causing defects in assembly, rotation, and switching of the flagellar motor, *J. Bacteriol. 175*, 802−810.
21. Sockett, H., Yamaguchi, S., Kihara, M., Irikura, V. M., and Macnab, R. M. (1992) Molecular analysis of the flagellar switch protein FliM of *Salmonella typhimurium*, *J. Bacteriol. 174*, 793−806.
22. Jones, C. J., and Macnab, R. M. (1990) Flagellar assembly in *Salmonella typhimurium*: Analysis with temperature-sensitive mutants, *J. Bacteriol. 172*, 1327−1339.
23. Vogler, A. P., Homma, M., Irikura, V. M., and Macnab, R. M. (1991) *Salmonella typhimurium* mutants defective in flagellar filament regrowth and sequence similarity of FliI to $F_0F_1$, vacuolar, and archaebacterial ATPase subunits, *J. Bacteriol. 173*, 3564−3572.
24. Jackson, M. W., and Plano, G. V. (2000) Interactions between type III secretion apparatus components from *Yersinia pestis* detected using the yeast two-hybrid system, *FEMS Microbiol. Lett. 186*, 85−90.
25. Jouihri, N., Sory, M.-P., Page, A.-L., Gounon, P., Parsot, C., and Allaoui, A. (2003) MxiK and MxiN interact with the Spa47 ATPase and are required for transit of the needle components MxiH and MxiI, but not of Ipa proteins, through the type III secretion apparatus of *Shigella flexneri*, *Mol. Microbiol. 49*, 755−767.
26. Fadouloglou, V. E., Tampakaki, A. P., Glykos, N. M., Bastaki, M. N., Hadden, J. M., Phillips, S. E., Panopoulos, N. J., and Kokkinidis, M. (2004) Structure of HrcQB−C, a conserved component of the bacterial type III secretion systems, *Proc. Natl. Acad. Sci. U.S.A. 101*, 70−75.
27. González-Pedrajo, B., Minamino, T., Kihara, M., and Namba, K. (2006) Interactions between C ring proteins and export apparatus components: a possible mechanism for facilitating flagellar type III protein export, *Mol. Microbiol. 60*, 984−998.
28. Woo, T. H. S., Cheng, A. F., and Ling, J. M. (1992) An application of a simple method for the preparation of bacterial DNA, *BioTechniques 13*, 696−698.
29. Toker, A. S., Kihara, M., and Macnab, R. M. (1996) Deletion analysis of the FliM flagellar switch protein of *Salmonella typhimurium*, *J. Bacteriol. 178*, 7069−7079.
30. Dreyfus, G., Williams, A. W., Kawagishi, I., and Macnab, R. M. (1993) Genetic and biochemical analysis of *Salmonella typhimurium* FliI, a flagellar protein related to the catalytic subunit of $F_0F_1$ ATPase and to virulence proteins of mammalian and plant pathogens, *J. Bacteriol. 175*, 3131−3138.
31. Ohnishi, K., Ohto, Y., Aizawa, S.-I., Macnab, R. M., and Iino, T. (1994) FlgD is a scaffolding protein needed for flagellar hook assembly in *Salmonella typhimurium*, *J. Bacteriol. 176*, 2272−2281.
32. Minamino, T., González-Pedrajo, B., Kihara, M., Namba, K., and Macnab, R. M. (2003) The ATPase FliI can interact with the type III flagellar protein export apparatus in the absence of its regulator, FliH, *J. Bacteriol. 185*, 3983−3988.
33. Morita-Ishihara, T., Ogawa, M., Sagara, H., Yoshida, M., Katayama, E., and Sasakawa, C. (2006) *Shigella* Spa33 is an essential C-ring component of type III secretion machinery, *J. Biol. Chem. 281*, 599−607.
34. Claret, L., Calder, S. R., Higgins, M., and Hughes, C. (2003) Oligomerization and activation of the FliI ATPase central to bacterial flagellum assembly, *Mol. Microbiol. 48*, 1349−1355.
35. Paul, K., and Blair, D. F. (2006) Organization of FliN subunits in the flagellar motor of *Escherichia coli*, *J. Bacteriol. 188*, 2502−2511.
36. Katayama, E., Shiraishi, T., Oosawa, K., Baba, N., and Aizawa, S.-I. (1996) Geometry of the flagellar motor in the cytoplasmic membrane of *Salmonella typhimurium* as determined by stereophotogrammetry of quick-freeze deep-etch replica images, *J. Mol. Biol. 255*, 458−475.
37. Minamino, T., and Macnab, R. M. (2000) Interactions among components of the *Salmonella* flagellar export apparatus and its substrates, *Mol. Microbiol. 35*, 1052−1064.
38. Francis, N. R., Sosinsky, G. E., Thomas, D., and DeRosier, D. J. (1994) Isolation, characterization and structure of bacterial flagellar motors containing the switch complex, *J. Mol. Biol. 235*, 1261−1270.
39. Minamino, T., Chu, R., Yamaguchi, S., and Macnab, R. M. (2000) Role of FliJ in flagellar protein export in *Salmonella*, *J. Bacteriol. 182*, 4207−4215.
40. Fraser, G. M., González-Pedrajo, B., Tame, J. R. H., and Macnab, R. M. (2003) Interactions of FliJ with components of the *Salmonella* type III flagellar export apparatus, *J. Bacteriol. 185*, 5546−5554.
41. Thomas, J., Stafford, G. P., and Hughes, C. (2004) Docking of cytosolic chaperone−substrate complexes at the membrane ATPase during flagellar type III protein export, *Proc. Natl. Acad. Sci. U.S.A. 101*, 3945−3950.
42. Auvray, F., Ozin, A. J., Claret, L., and Hughes, C. (2002) Intrinsic membrane targeting of the flagellar export ATPase FliI: Interaction with acidic phospholipids and FliH, *J. Mol. Biol. 318*, 941−950.
43. Ryu, J., and Hartin, R. J. (1990) Quick transformation in *Salmonella typhimurium* LT2, *BioTechniques 8*, 43−44.
44. Yamaguchi, S., Fujita, H., Sugata, K., Taira, T., and Iino, T. (1984) Genetic analysis of *H2*, the structural gene for phase-2 flagellin in *Salmonella*, *J. Gen. Microbiol. 130*, 255−265.
45. Van Arnam, J. S., McMurry, J. L., Kihara, M., and Macnab, R. M. (2004) Analysis of an engineered *Salmonella* flagellar fusion protein, FliR−FlhB, *J. Bacteriol. 186*, 2495−2498.
46. Amman, E., Ochs, B., and Karl-Josef, A. (1988) Tightly regulated *tac* promoter vectors useful for the expression of unfused and fused proteins in *Escherichia coli*, *Gene 69*, 310−315.
47. Ohnishi, K., Fan, F., Schoenhals, G. J., Kihara, M., and Macnab, R. M. (1997) The FliO, FliP, FliQ, and FliR proteins of *Salmonella typhimurium*: Putative components for flagellar assembly, *J. Bacteriol. 179*, 6092−6099.

BI0605890